Eur. J. Mech. B/Fluids, **18**, n° 2, 245-260, 1999

Analysis of the transpiration cooling of a thin porous plate in a hot laminar convective flow

C. TREVIÑO [a]*, A. MEDINA [b]

ABSTRACT. – This paper deals with the asymptotic and numerical analysis for the steady-state transpiration cooling of a thin porous flat plate in a laminar hot convective flow, taking into account the streamwise heat conduction through the plate. For high conductivity plates, a regular perturbation analysis has been carried out, yielding a three-term asymptotic solution for the distribution of plate temperature. In the limit of a very poorly conducting plate, a singular perturbation technique, based on matched asymptotic expansions, is employed to solve the governing equations. We also solved the equations numerically using a quasilinearization technique. The numerical results are in good agreement with the asymptotic solution close to the asymptotic limits studied. © Elsevier, Paris.

Nomenclature

Symbol definition

B	injection parameter defined by $B = \int_0^1 \beta(\chi)d\chi$
c	specific heat of the injected and hot fluids
f	nondimensional stream function for the fluid defined in eq. (15)
G_0	nondimensional temperature gradient introduced in eq. (26)
G_1	nondimensional temperature gradient introduced in eq. (42)
g_1	nondimensional variable introduced in eq. (29)
H	internal heat transfer coefficient introduced in eq. (8)
h	half-thickness of the plate
K	nondimensional variable defined by $K = \varepsilon^2 \Pr \beta/\alpha$
L	length of the plate
m	injection distribution parameter defined with $\beta = B(1+m)\chi^m$
Pr	Prandtl number of the fluid, $\Pr = \mu c/\lambda$
Re_∞	Reynolds number of the flow, $Re_\infty = U_\infty L/\nu$

Greek symbols

α	heat conduction parameter defined in eq. (6)
β	injection function defined in eq. (3)
γ	internal heat transfer parameter defined by $\gamma = Hh/(\rho c \overline{V}_c)$
η	nondimensional coordinate defined in eq. (15)
χ	nondimensional longitudinal coordinate, $\chi = x/L$
ε	aspect ratio of the plate, $\varepsilon = h/L$
λ	thermal conductivity of the fluid
λ_w	thermal conductivity of the plate
μ	dynamic viscosity of the fluid
ν	kinematic viscosity of the fluid
φ_w	nondimensional variable defined in eq. (49)
φ_1	nondimensional variable introduced in eq. (30)
ψ	stream function defined after eq. (16)
θ	nondimensional temperature of the fluid defined in eq. (15)
θ_g	nondimensional temperature of the injected fluid defined in eq. (15)

* Correspondence and reprints.
[a] Facultad de Ciencias, UNAM, 04510 México D. F., Mexico. Email: ctrev@servidor.unam.mx
[b] Subdirección de Exploración y Producción, Instituto Mexicano del Petróleo, Eje Central Lázaro Cárdenas 152, 07730 México D. F., Mexico.

0997-7546/99/02/© Elsevier, Paris

T temperature of the fluid
T_∞ temperature of the hot fluid
T_c initial temperature of the cooling fluid
T_g temperature of the cooling fluid
T_w temperature of the plate
u longitudinal velocity component of the fluid
U_∞ free stream velocity of the hot fluid
v transverse velocity component of the fluid
V_c injection velocity of the cooling fluid
x, y horizontal and vertical Cartesian coordinates
z nondimensional transverse coordinate for the plate, $z = y/h$
θ_w nondimensional plate temperature defined in eq. (14)
ξ nondimensional longitudinal coordinate defined in eq. (49)

Subscripts

$0, 1, 2$ denotes the leading, first or second order solution
c denotes the initial temperature of the cooling fluid
g denotes the cooling fluid
w denotes the plate
∞ conditions at the hot free stream

1. Introduction

One of the most important problems in gas turbine development is that related to the increased efficiency obtained by increasing the working temperature at the exit of the combustion chamber. However, this maximum temperature is limited by the blade material. Transpiration cooling can be used in this case to reduce the temperature of the blade in contact with very hot gases, thus increasing the working temperature and therefore the cycle efficiency (Polezhaev, 1997). The injected cooling fluid extracted directly from the final rows of the compressor section travels through the porous material, being heated first by the wall and later by mixing with the hot fluid. There are also multiple applications for transpiration cooling processes, which can be inferred from the following references (Modlin and Colwell, 1992, Xu and Yang, 1993, Sreekanth and Reddy, 1995, Shunichi, 1996).

Transpiration cooling processes involve simultaneously two different heat transfer mechanisms: conduction through a solid plus convection. There is a large amount of literature in this field of conjugate heat transfer processes (Luikov, 1974, Payvar, 1977, Treviño and Liñán, 1984, Pozzi and Lupo, 1988, Higuera and Pop, 1997, among others). In particular, the effect of wall transpiration on the heat transfer process, has been studied numerically in several works (Hartnett and Eckert, 1957; Hartnett *et al.*, 1961; Cheng, 1977; Minkowycz *et al.*, 1985 and Lai and Kulacki, 1990). Brouwers in a recent paper (Brouwers, 1994) studied the heat and mass transfer between a permeable wall and a porous medium, including the effect of injection and suction on the process. He uses the so called film model, which is an approximation of the boundary layer flow. For an injection parameter of $B = 0.5$, he obtained a relatively good correlation with an accuracy of 95%, as compared with the boundary layer model. Eckert and Cho, (1994) (see also Brouwers, 1995), obtained numerically the heat transfer characteristics of a porous wall in a turbulent boundary layer flow, using the $k - \varepsilon$ model. In none of these works has the streamwise heat conduction through the porous material been considered.

The objective of the present work is to study both numerically and using asymptotic techniques, the influence of the injection of a cooling fluid through a porous plate in contact with a laminar convective flow of a hot fluid. The streamwise heat conduction through the wall is considered for the different regimes. In section 2 we present order of magnitude estimates for the studied process and the corresponding governing equations. In section 3 we present the asymptotic solution for the thermally thin wall regime. The solution for the thermally thick wall regime is given in section 4. The most important results and the influence of the injection strength and the distribution of the injected fluid upon the maximum temperature in the plate are given in section 5. Finally we present the key conclusions in section 6.

2. Formulation

The physical model analyzed, depicted in figure 1, is the following. A thin porous flat plate of length L and thickness h is placed parallel to the forced flow of an incompressible fluid with free stream velocity U_∞ and temperature T_∞. A transpiration cooling flow is added through the porous plate, with a known temperature $T_c < T_\infty$ and injection velocity $V_c(x)$. In this paper, heat conduction in both directions is considered while both ends of the plate are assumed, for simplicity, to be adiabatic. The order of magnitude of the characteristic thickness of the boundary layer flow δ is obtained from the balance of the viscous and inertial forces, together with mass conservation as

$$\frac{\nu U_\infty}{\delta^2} \sim \frac{U_\infty^2}{L}; \quad \frac{U_\infty}{L} \sim \frac{V}{\delta}, \tag{1}$$

where ν is the kinematic viscosity of the fluid and V denotes the characteristic transverse velocity component induced by the boundary layer flow. Therefore, the boundary layer thickness related to the length of the plate must be of the order

$$\frac{\delta}{L} \sim \frac{1}{Re_\infty^{1/2}} \sim \frac{V}{U_\infty}, \tag{2}$$

where Re_∞ is the Reynolds number based on the free-stream velocity, defined by $Re_\infty = U_\infty L/\nu$. The relative importance of the injection process on the boundary layer flow is represented by the injection parameter

$$\beta = \frac{Re_c}{Re_\infty^{1/2}} = \frac{V_c Re_\infty^{1/2}}{U_\infty} \sim \frac{\overline{V_c}}{V} \tag{3}$$

where Re_c is the Reynolds number based on the injection velocity, $Re_c = \overline{V_c} L/\nu$. Here $\overline{V_c}$ is the averaged value of the injection velocity, $\overline{V_c} = \int_0^L V_c dx/L$. The value of β must be lower than the critical value needed for boundary layer separation, which is of order unity. Assuming that the injected fluid at the exit equilibrates the fluid temperature with that of the solid, we obtain from the energy equation

$$\frac{(T_\infty - T_w)}{\delta_T} \sim \frac{\mathrm{Pr}\, V_c}{\nu}(T_c - T_w) \sim \frac{\lambda_w \Delta T_w}{\lambda h}, \tag{4}$$

where δ_T is the characteristic thickness of the thermal boundary layer, and is of order $\delta_T \sim \delta/\mathrm{Pr}^{1/3}$, for $\mathrm{Pr} \gg 1$. $Pr = \rho\nu c/\lambda$ is the Prandtl number. Here ΔT_w is the characteristic temperature difference in the transverse direction, T_w is the characteristic averaged value of the temperature of the plate, λ_w and λ are

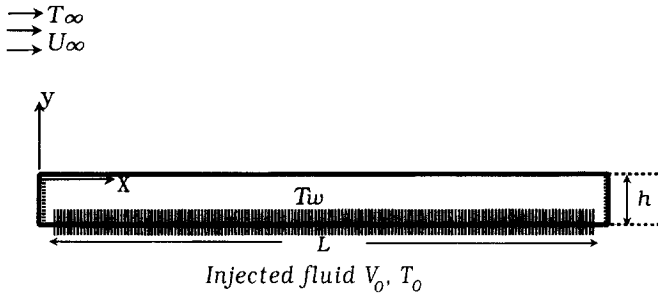

Fig. 1. – Schematic of the physical problem studied.

the thermal conductivity of the plate and fluid, respectively and c is the specific heat at constant pressure of the fluid. Therefore, the characteristic temperature difference in the transverse direction related to the overall temperature difference $T_\infty - T_w$ can be written as

$$\frac{\Delta T_w}{(T_\infty - T_w)} \sim \frac{\varepsilon^2}{\alpha} Pr^{1/3} \sim \frac{\varepsilon^2 \beta \,\mathrm{Pr}}{\alpha} \frac{(T_c - T_w)}{(T_\infty - T_w)}, \tag{5}$$

where the parameter α corresponds to the nondimensional longitudinal thermal conductance of the wall and is defined by

$$\alpha = \frac{\lambda_w}{\lambda} \frac{h}{L} \frac{1}{Re_\infty^{1/2}}, \tag{6}$$

and ε is the aspect ratio of the plate, $\varepsilon = h/L$. For large values of α/ε^2, the nondimensional temperature of the plate can be given globally by

$$T_w \sim \frac{T_\infty + \beta \,\mathrm{Pr}^{2/3} T_c}{1 + \beta \,\mathrm{Pr}^{2/3}}; \quad \frac{\Delta T_w}{(T_\infty - T_w)} \to 0. \tag{7}$$

For $\beta \ll 1$, the plate temperature is of the order $T_w \sim T_\infty - \beta \,\mathrm{Pr}^{2/3}(T_\infty - T_c)$. Increasing the value of the injection parameter produces a decrease in the plate temperature. The transverse temperature gradient produced in the cooling process in this regime is $\nabla T_y \sim (\varepsilon/\alpha)(T_\infty - T_c)/L$. The corresponding longitudinal component is then $\nabla T_x \sim (1/\alpha)(T_\infty - T_c)/L$, for values of α of order unity or larger and $\nabla T_x \sim \Delta T_c/L$, otherwise. Larger temperature gradients are produced in the longitudinal direction for values of $\alpha > \varepsilon$. On the other hand, for values of α/ε^2 of order unity, called the thermally thick wall approximation, the wall temperature variations in the transverse direction are now important and this effect must be included in the analysis. In this limit, the longitudinal heat conduction through the plate now is unable to compete with the convective heat flux towards the fluid and can be neglected in a first approximation. In this regime, the transverse temperature gradient generated during the cooling process is much larger than the corresponding longitudinal gradients and is of order $\nabla T_y \sim (1/\varepsilon)\Delta T_c/L$.

The energy balance equation for the plate can be written as

$$\frac{\partial^2 T_w}{\partial x^2} + \frac{\partial^2 T_w}{\partial y^2} - \frac{H}{\lambda_w}(T_w - T_g) = 0, \tag{8}$$

where H is a volumetric heat transfer coefficient between the plate and the injected fluid, with a local temperature T_g. The governing equation for the injected fluid is then

$$H(T_w - T_g) = \rho_g c_g V_c \frac{\partial T_g}{\partial y}, \tag{9}$$

where ρ_g, c_g are the density and the specific heat of the injected fluid. We assume for simplicity that the injected fluid and the hot fluid are the same and are assumed to be incompressible. This latter restriction can be easily removed by introducing the Howarth-Dorodnizyn transformation (Schlichting, 1979), which allow us to transform the compressible flow problem to incompressible boundary layer governing equations. The boundary conditions are given by

$$\frac{\partial T_w}{\partial x} = 0 \quad \text{at } x = 0, x = L;$$

$$\lambda_w \frac{\partial T_w}{\partial y} - \lambda \frac{\partial T}{\partial y} - \rho V_c c(T_g - T_w) = 0 \quad \text{at } y = 0;$$

$$\frac{\partial T_w}{\partial y} = T_g - T_c = 0 \quad \text{at } y = -h. \tag{10}$$

The governing equations for the incompressible hot fluid, using the boundary layer approximation, are given by

$$\frac{\partial u}{\partial x} + \frac{\partial v}{\partial y} = 0, \tag{11}$$

$$u\frac{\partial u}{\partial x} + v\frac{\partial u}{\partial y} = \nu \frac{\partial^2 u}{\partial y^2}, \tag{12}$$

where u and v correspond to the longitudinal and transverse velocity components, respectively. The boundary conditions are

$$u = v - V_c = 0 \quad \text{at } y = 0; \; u \to U_\infty \quad \text{as } y \to \infty. \tag{13}$$

Introducing the following nondimensional variables

$$\theta_w = \frac{(T_w - T_c)}{(T_\infty - T_c)}; \quad \chi = \frac{x}{L}; \quad z = \frac{y}{h} \tag{14}$$

$$\theta_g = \frac{(T_g - T_c)}{(T_\infty - T_c)}; \quad \theta = \frac{(T - T_c)}{(T_\infty - T_c)}; \quad \eta = \sqrt{\frac{U_\infty}{\nu x}}\, y; \quad f = \frac{\psi}{\sqrt{U_\infty \nu x}}, \tag{15}$$

eqs. (8) and (9) take the nondimensional form

$$\frac{\partial^2 \theta_w}{\partial \chi^2} + \frac{1}{\varepsilon^2}\frac{\partial^2 \theta_w}{\partial z^2} - \frac{Pr\beta\gamma}{\alpha}(\theta_w - \theta_g) = 0; \quad \gamma(\theta_w - \theta_g) = \frac{\partial \theta_g}{\partial z}. \tag{16}$$

Here, ψ is the classical stream function defined by $u = \partial\psi/\partial y$ and $v = -\partial\psi/\partial x$. γ is the internal heat transfer parameter defined as $\gamma = Hh/(\rho c \overline{V_c})$. For large values of γ compared with unity, the injection fluid temperature rapidly reaches the temperature of the plate, which allow us to write $\theta_g = \theta_w$ at $z = 0$ for $\gamma \gg 1$. The nondimensional governing equations for the hot fluid take the classical form (Schlichting, 1979)

$$\frac{\partial^3 f}{\partial \eta^3} + \frac{f}{2}\frac{\partial^2 f}{\partial \eta^2} = \chi\left[\frac{\partial f}{\partial \eta}\frac{\partial^2 f}{\partial \chi \partial \eta} - \frac{\partial f}{\partial \chi}\frac{\partial^2 f}{\partial \eta^2}\right], \tag{17}$$

$$\frac{1}{\mathrm{Pr}}\frac{\partial^2 \theta}{\partial \eta^2} + \frac{f}{2}\frac{\partial \theta}{\partial \eta} = \chi\left[\frac{\partial f}{\partial \eta}\frac{\partial \theta}{\partial \chi} - \frac{\partial f}{\partial \chi}\frac{\partial \theta}{\partial \eta}\right], \tag{18}$$

with the boundary conditions

$$f(0) + 2\sqrt{\chi}\beta(\chi) = \frac{\partial \theta_w}{\partial z} - \frac{\varepsilon^2}{\alpha}\left[\frac{1}{\sqrt{\chi}}\frac{\partial \theta}{\partial \eta} - \beta Pr(\theta_w - \theta_g)\right]$$

$$= \frac{\partial f}{\partial \eta} = \theta - \theta_w = 0 \quad \text{at } \eta = 0, \tag{19}$$

$$\frac{\partial f}{\partial \eta} - 1 = \theta - 1 = 0 \quad \text{at } \eta \to \infty. \tag{20}$$

Here the injection function $\beta(\chi) = V_c\sqrt{Re_\infty}/U_\infty$ is assumed to be a function of the longitudinal coordinate χ. We introduce the normalized function $\widetilde{\beta}(\chi) = \beta(\chi)/B$, such as $\int_0^1 \widetilde{\beta}(\chi)d\chi = 1$. B is then the strength of

the injection process. In the following section we present a solution in the limit $\alpha/\varepsilon^2 >> 1$, which is called the thermally thin wall regime, where the temperature variations in the transverse direction of the plate can be neglected. It is in this regime where the transpiration cooling produces the most important benefits, due to a reduction of the maximum temperature in the plate without the appearance of serious wall temperature gradients.

3. Thermally thin wall regime ($\alpha/\varepsilon^2 >> 1$)

In this regime, the non-dimensional transverse temperature variations in the plate are very small, of order ε^2/α as predicted by relationship (5). Integrating the energy equation across the solid and applying the boundary conditions, we obtain a reduced form of the nondimensional energy equation for the plate as

$$\alpha \frac{d^2\theta_w}{d\chi^2} + \frac{1}{\sqrt{\chi}} \left.\frac{\partial\theta}{\partial\eta}\right|_{\eta=0} - \Pr \beta\theta_w = 0. \tag{21}$$

In this regime the final equation is independent of γ, for large values of γ. In this case, the temperature of the cooling fluid reaches the temperature of the plate at the exit. Here we obtain the lowest values of the temperature gradients in the plate, being of order $(T_\infty - T_c)/(\alpha L)$, valid for values of α of order unity or larger. For values of $\alpha >> 1$, the temperature of the plate equilibrates due to its large thermal conductivity. In this limit the temperature gradients at the wall are very small and the maximum temperature at the plate is the lowest possible using this kind of cooling process.

3.1. Asymptotic limit $\alpha >> 1$

For very large values of the parameter α compared with unity, the nondimensional temperature of the plate changes very little, of order α^{-1} in the longitudinal direction. This limit is regular and is to be analyzed using α^{-1} as the small expansion parameter. In this limit, the nondimensional temperature of the plate can be obtained using the following asymptotic series

$$\theta_w(\alpha, \chi) = \sum_{n=0}^{\infty} \frac{1}{\alpha^n} \theta_{wn}(\chi). \tag{22}$$

Introducing the above relationship into the nondimensional governing eq. (21), we obtain the following set of equations

$$\frac{d^2\theta_{w0}}{d\chi^2} = 0, \tag{23}$$

$$\frac{d^2\theta_{wn}}{d\chi^2} = -\frac{1}{\sqrt{\chi}} \left.\frac{\partial\theta_{n-1}}{\partial\eta}\right|_{\eta=0} + \Pr \beta\theta_{w(n-1)} \quad \text{for } n \geq 1, \tag{24}$$

with the following adiabatic conditions at both ends

$$\frac{d\theta_{wn}}{d\chi} = 0 \quad \text{at } \chi = 0, 1 \quad \text{for all } n. \tag{25}$$

Solving equations (23) and (25), gives a constant value for θ_{w0}, which can be found after integrating the following first order eq. (24) with the corresponding adiabatic conditions at both ends as

$$\int_0^1 \frac{d^2\theta_{w1}}{d\chi^2} d\chi = 0 = -\int_0^1 \frac{1}{\sqrt{\chi}} \left.\frac{d\theta_0}{d\eta}\right|_{\eta=0} d\chi + \Pr B\theta_{w0}.$$

In this form, the solution for θ_{w0} is given by

$$\theta_{w0} = \left[1 + \frac{PrB}{2\overline{G_0}(m, B, Pr)}\right]^{-1}; \quad \overline{G_0} = \frac{1}{2}\int_0^1 \frac{G_0 d\chi}{\sqrt{\chi}}. \tag{26}$$

Here $G_0(\chi; m, B, Pr)$ corresponds to the nondimensional temperature gradient at the surface of the wall obtained from eqs. (17) and (18), with the normalized conditions $\theta_0 = 0$ at $\eta = 0$ and $\theta_0 = 1$ as $\eta \to \infty$. In this case, we represent the normalized injection function as $\widetilde{\beta}(\chi) = (1+m)\chi^m$, where m denotes the distribution parameter of the injection process. Any other function can be included without any difficulty. A first integration of Eq. (24) for $n = 1$, gives

$$\frac{d\theta_{w1}}{d\chi} = 2\overline{G_0}(1 - \theta_{w0})\left[\chi^{m+1} - \frac{1}{2\overline{G_0}}\int_0^{\backslash} \frac{G_0 d\chi}{\sqrt{\chi}}\right]. \tag{27}$$

For $m = -1/2$, we obtain that $\theta_{wn} = 0$ for all $n > 0$. For this specific injection function, the leading order solution is valid for all values of α. A second integration of Eq. (27) gives

$$\theta_{w1} = C_1 + 2\overline{G_0}(1 - \theta_{w0})\left[\frac{\chi^{m+2}}{m+2} - \frac{1}{2\overline{G_0}}\int_0^{\backslash} d\chi \int_0^{\backslash} \frac{G_0 d\overline{\chi}}{\sqrt{\overline{\chi}}}\right], \tag{28}$$

where C_1 can be obtained by solving the second order equation (24) for $m = 2$. For $B \ll 1$, from eq. (26) and assuming a solution of the form

$$f_0 = f_{00} + 2B\chi^{m+1/2}(1+m)(-1+g_1) + O(B^2), \tag{29}$$

$$\theta_0 = \theta_{00} + 2B\chi^{m+1/2}(m+1)\varphi_1 + O(B^2), \tag{30}$$

we obtain at leading order

$$\frac{d^3 f_{00}}{d\eta^3} + \frac{f_{00}}{2}\frac{d^2 f_{00}}{d\eta^2} = 0; \quad \frac{d^2\theta_{00}}{d\eta^2} + \frac{\mathrm{Pr}\, f_{00}}{2}\frac{d\theta_{00}}{d\eta} = 0, \tag{31}$$

with the well known asymptotic solution obtained for large Prandtl numbers, but which gives excellent results for values of order unity, given by

$$\theta_{00} = 0.7765 \int_0^{(\frac{\mathrm{Pr}\, f''(0)}{4})^{1/3}\eta} \exp\left[\frac{-t^3}{3}\right] dt \text{ with } f''(0) = 0.332. \tag{32}$$

The first order equations take the form

$$\frac{d^3 g_1}{d\eta^3} + \frac{f_{00}}{2}\frac{d^2 g_1}{d\eta^2} - \left(m + \frac{1}{2}\right)\frac{df_{00}}{d\eta}\frac{dg_1}{d\eta} + (m+1)\frac{d^2 f_{00}}{d\eta^2} g_1 = (m+1)\frac{d^2 f_{00}}{d\eta^2}, \tag{33}$$

$$\frac{1}{\mathrm{Pr}}\frac{d^2\varphi_1}{d\eta^2} + \frac{f_{00}}{2}\frac{d\varphi_1}{d\eta} - \left(m + \frac{1}{2}\right)\frac{df_{00}}{d\eta}\varphi_1 + (m+1)\frac{d\theta_0}{d\eta} g_1 = (m+1)\frac{d\theta_0}{d\eta}, \tag{34}$$

to be solved with the boundary conditions

$$g_1 = \frac{dg_1}{d\eta} = \varphi_1 = 0 \quad \text{at } \eta = 0; \quad \frac{dg_1}{d\eta} = \varphi_1 = 0 \quad \text{for } \eta \to \infty. \tag{35}$$

The nondimensional temperature gradient then is given by

$$G_0 = G_{00} + 2B(m+1)\chi^{m+1/2}G_{01}, \tag{36}$$

where

$$G_{00} = \left.\frac{d\theta_{00}}{d\eta}\right|_{\eta=0} = 0.3387\,\mathrm{Pr}^{1/3} \text{ and } G_{01}(m,Pr) = \left.\frac{d\varphi_1}{d\eta}\right|_{\eta=0}. \tag{37}$$

The averaged value of the nondimensional temperature gradient is up to the first order terms

$$\overline{G_0} = G_{00} + BG_{01} + O(B^2). \tag{38}$$

By using eq. (26) and the previous result we obtain

$$\theta_{w0} = \left[1 - \frac{\mathrm{Pr}\,B}{2G_{00}} + \frac{\mathrm{Pr}^2 B^2}{4G_{00}^2}\left(1 + \frac{2G_{01}(m,Pr)}{Pr}\right) + O(B^3)\right]. \tag{39}$$

Figure 2 shows the leading order solution θ_{w0} obtained numerically, as a function of the injection strength B, for a Prandtl number of unity and different values of m. The asymptotic solution, up to terms of order B, given by eq. (39) for $m = 0$, is also plotted. This approximation is enough to describe with acceptable accuracy the leading order solution. Figures 3 and 4 show the numerically obtained function G_{01} for different values of Pr and m, respectively. This function can be well correlated by

$$G_{01} \simeq -1.212 - 1.0487m + 0.436m^2 - 1.1072(\mathrm{Pr} - 1), \tag{40}$$

for values of $\mathrm{Pr} \sim 1$. Therefore, up to the second order, θ_{w1} is given by

$$\theta_{w1} = C_1 + BPr\left[\frac{\chi^{m+2}}{m+2} - \frac{2}{3}\chi^{3/2}\right] + O(B^2). \tag{41}$$

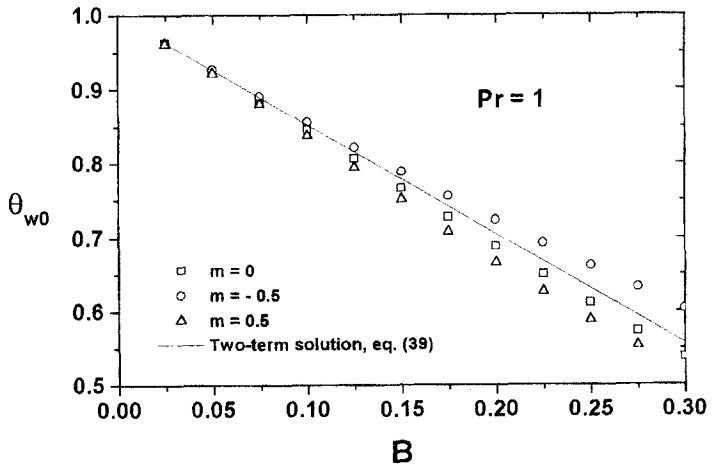

Fig. 2. – Leading order solution for the nondimensional plate temperature, θ_{w0}, obtained numerically, as a function of the injection strength B and three different values of m. The Prandtl number is $\mathrm{Pr} = 1$. The two-term asymptotic solution given by eq. (39) for $m = 0$ is also plotted.

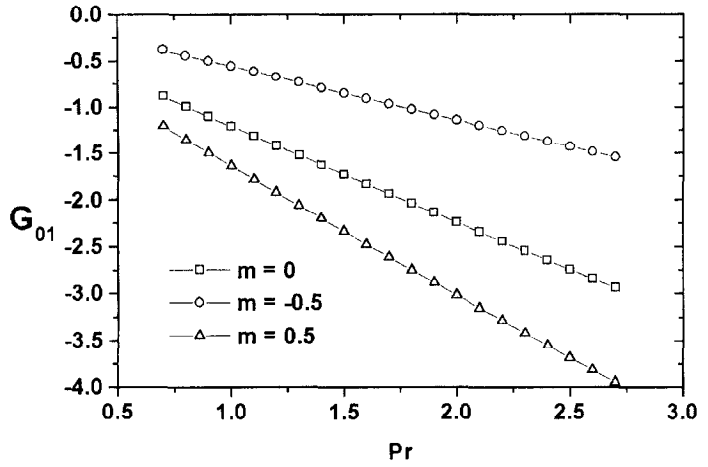

Fig. 3. – First order nondimensional temperature gradient, G_{01}, as a function of the Prandtl number for three different values of m.

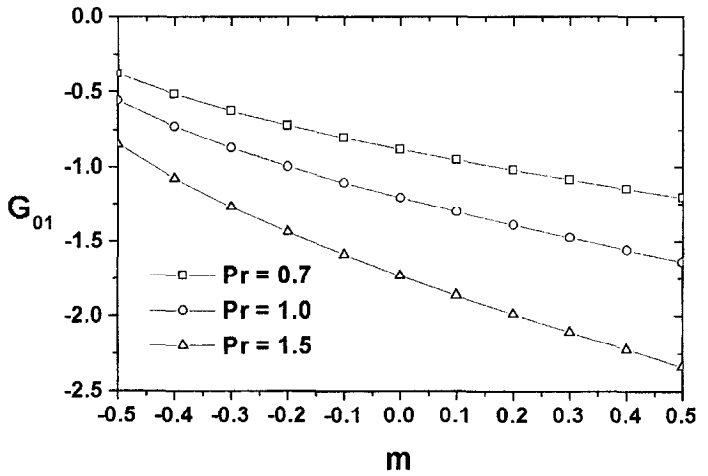

Fig. 4. – First order nondimensional temperature gradient, G_{01}, as a function of m, for three different values of the Prandtl number.

After evaluating the constant C_1 by integrating the second order equation (24), we obtain the second order result

$$\theta_w = \left\{1 - \frac{\mathrm{Pr}\,B}{2G_{00}} + \frac{\mathrm{Pr}^2\,B^2}{4G_{00}^2}\left(1 + \frac{2G_{01}(m,Pr)}{Pr}\right)\right.$$

$$\left. + \frac{\mathrm{Pr}\,B}{\alpha 2G_{00}}\left[\frac{G_1(m+2)}{(m+2)(m+5/2)} - \frac{G_1(3/2)}{3} + 2G_{00}\left(\frac{\chi^{m+2}}{m+2} - \frac{2}{3}\chi^{3/2}\right)\right]\right\}$$

$$+ O(B^2/\alpha, B^3), \tag{42}$$

where G_1, found using the Lighthill approximation (Lighthill, 1950), is given by

$$G_1(n) = -\frac{4nG_{00}}{3}\frac{\Gamma(4n/3)\Gamma(2/3)}{\Gamma(4n/3+2/3)},$$

where $\Gamma(z)$ corresponds to the Gamma function.

3.2. Asymptotic limit $\alpha \to 0$

In this limit we can neglect the streamwise heat conduction through the plate except in regions close to the ends. This longitudinal heat conduction has to be retained in these regions in order to achieve the adiabatic boundary conditions. The resulting equation for the outer region (where the streamwise heat conduction is neglected) is given by

$$\left.\frac{\partial\theta}{\partial\eta}\right|_{\eta=0} = \zeta\theta_w \text{ with } \zeta = BPr(1+m)\chi^{m+1/2}. \tag{43}$$

The governing equations for the fluid now take the form

$$\frac{\partial^3 f}{\partial\eta^3} + \frac{f}{2}\frac{\partial^2 f}{\partial\eta^2} = \zeta(m+\frac{1}{2})\left[\frac{\partial f}{\partial\eta}\frac{\partial^2 f}{\partial\zeta\partial\eta} - \frac{\partial f}{\partial\zeta}\frac{\partial^2 f}{\partial\eta^2}\right], \tag{44}$$

$$\frac{1}{\mathrm{Pr}}\frac{\partial^2\theta}{\partial\eta^2} + \frac{f}{2}\frac{\partial\theta}{\partial\eta} = \zeta(m+\frac{1}{2})\left[\frac{\partial f}{\partial\eta}\frac{\partial\theta}{\partial\zeta} - \frac{\partial f}{\partial\zeta}\frac{\partial\theta}{\partial\eta}\right], \tag{45}$$

with the boundary conditions

$$f(0) + \frac{2\zeta}{Pr} = \frac{\partial\theta}{\partial\eta} - \zeta\theta = \theta_w - \theta = \frac{\partial f}{\partial\eta} = 0 \quad \text{at } \eta = 0,$$

$$\frac{\partial f}{\partial\eta} - 1 = \theta - 1 = 0 \quad \text{at } \eta \to \infty. \tag{46}$$

For large values of the Prandtl number, the limiting behavior can be obtained after neglecting the injection process for the momentum equation (44), reducing the fluid equations to the classical form solved by Lighthill (1950), viz.

$$\frac{\partial\theta}{\partial\eta} = \left(\frac{f''(0)Pr}{4}\right)^{1/3}\int_1^{\theta_w} K_m d\theta'_w, \text{ where } K_m = \left[1 - \left(\frac{\zeta'}{\zeta}\right)^{3/(4(m+1/2))}\right]^{-1/3}. \tag{47}$$

Therefore, $\theta_w(\bar{\zeta})$ can be obtained after solving the integral equation

$$\int_1^{\theta_w} K_m d\theta'_w = -\bar{\zeta}\theta_w \text{ with } \bar{\zeta} = \zeta\left(\frac{4}{f''(0)Pr}\right)^{1/3}. \tag{48}$$

Figure 5 shows the nondimensional temperature of the plate as a function of $\bar{\zeta}$, for different values of m, for large values of the Prandtl number.

Close to the upstream end, the heat conduction effects must be retained in a thin layer of order $\alpha^{2/3}$ in χ. Introducing the following inner variables

$$\theta_w = 1 - \left(\frac{4}{f''(0)}\right)^{1/3} Pr^{2/3}B(1+m)\alpha^{(2m+1)/3}\varphi_w; \quad \chi = \alpha^{2/3}\xi, \tag{49}$$

the inner equation transforms to

$$\xi^{1/2}\frac{d^2\varphi_w}{d\xi^2} = \varphi_{wl} + \int_{\varphi_{wl}}^{\varphi_w} K_m d\varphi'_w - \xi^{m+1/2}, \tag{50}$$

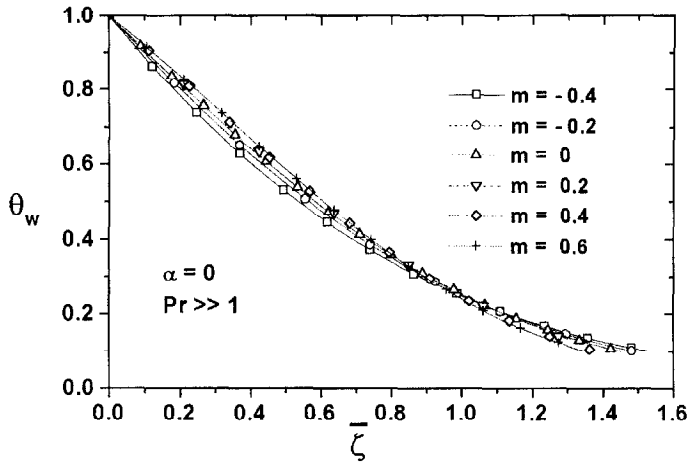

Fig. 5. – Nondimensional plate temperature as a function of $\bar{\zeta} = (4/f''(0))^{1/3} BPr^{2/3}(1+m)\chi^{m+1/2}$, for different values of m, obtained numerically in the limit $\alpha = 0$, for $\mathrm{Pr} \gg 1$.

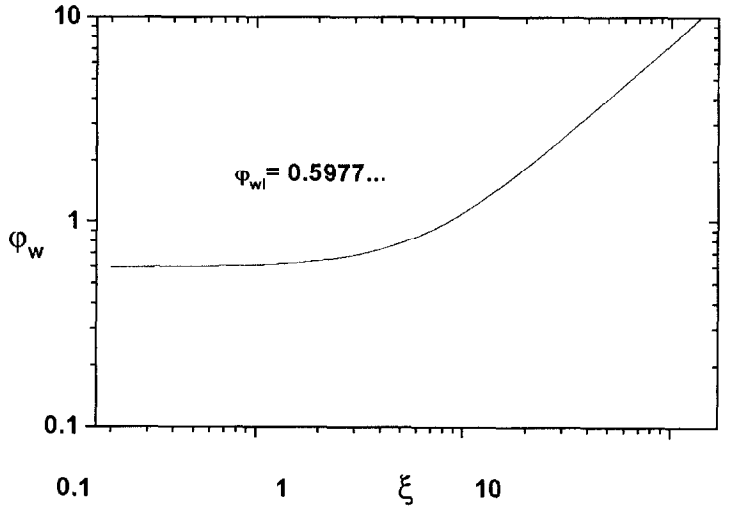

Fig. 6. – Inner region solution for $m = 1/2$.

with the boundary conditions

$$\frac{d\varphi_w}{d\xi} = 0 \quad \text{at } \xi = 0; \quad \varphi_w \sim a\xi^{m+1/2} \quad \text{for } \xi \to \infty. \tag{51}$$

Here φ_{wl} is the corresponding value of $\varphi_w(0)$ at the upstream end and

$$a = \frac{3}{4m+2} \frac{\Gamma(\frac{4m+4}{3})}{\Gamma(\frac{4m+2}{3})\Gamma(\frac{2}{3})}. \tag{52}$$

The last condition comes from matching with the outer solution. For $m = 1/2$, figure 6 shows the solution of eq. (50) for the inner region. Matching with the outer non-conducting region ($\xi \to \infty$, $\zeta \to 0$) can be obtained only for the unique value of $\varphi_{wl} \simeq 0.5977....$

4. Thermally thick wall regime

For values of $\alpha \sim \varepsilon^2 \ll 1$, the streamwise heat conduction through the wall is very small and can be neglected as mentioned for the case of $\alpha \to 0$ in subsection 3.2. However in this regime, the nondimensional temperature variation in the transverse direction of the plate now are of order unity and must be retained in the analysis. The nondimensional governing equations for the wall and the cooling fluid are then given by

$$\frac{\partial^2 \theta_w}{\partial z^2} = \frac{\varepsilon^2 \,\mathrm{Pr}\,\beta\gamma}{\alpha}(\theta_w - \theta_g) = \frac{\varepsilon^2 \,\mathrm{Pr}\,\beta}{\alpha}\frac{\partial \theta_g}{\partial z}, \tag{53}$$

with the initial and boundary conditions given by

$$\frac{\partial \theta_w}{\partial z} = \theta_g = 0 \quad \text{at } z = -1; \quad \frac{\partial \theta_w}{\partial z} = \frac{\varepsilon^2}{\alpha}\frac{1}{\sqrt{\chi}}\frac{\partial \theta}{\partial \eta}\bigg| \quad \text{at } z = 0. \tag{54}$$

From the first and third terms in eq. (53), together with eq. (54) we compute a first integration, resulting

$$\frac{\partial \theta_w}{\partial z} = \frac{\varepsilon^2 \,\mathrm{Pr}\,\beta}{\alpha}\theta_g. \tag{55}$$

Combining all three terms we obtain a single equation for θ_g of the form

$$\frac{\partial^2 \theta_g}{\partial z^2} + \gamma\frac{\partial \theta_g}{\partial z} - K\gamma\theta_g = 0, \tag{56}$$

where $K = \varepsilon^2 \,\mathrm{Pr}\,\beta/\alpha$. The solution can be readily obtained as

$$\theta_g = C_2 \exp\left(-\frac{\gamma(1+z)}{2}\right)\sinh\left(R(1+z)\right), \tag{57}$$

where $R = \gamma\sqrt{1 + 4K/\gamma}/2$. The constant C_2 is to be obtained from the boundary condition at $z = 0$. Using eq. (55) we also find

$$\theta_w = C_2 \exp\left(-\frac{\gamma(1+z)}{2}\right)\left[\frac{1}{2}\sinh(R(1+z)) + \frac{R}{\gamma}\cosh(R(1+z))\right]. \tag{58}$$

Therefore, the nondimensional temperature at the wall relative to that at the upper surface is then

$$\frac{\theta_w}{\theta_{wu}} = \exp\left(-\frac{\gamma z}{2}\right)\frac{\left[\frac{1}{2}\sinh(R(1+z)) + \frac{R}{\gamma}\cosh(R(1+z))\right]}{\left[\frac{1}{2}\sinh(R) + \frac{R}{\gamma}\cosh(R)\right]}, \tag{59}$$

where θ_{wu} is the nondimensional temperature of the plate at $z = 0$, which may be obtained in a similar form as in the limit $\alpha \to 0$ for the thermally thin wall regime (subsection 3.2.), by solving the integral equation

$$\int_1^{\theta_w} K_m d\theta'_{wu} = -\bar{\zeta}\theta_{wu}; \quad \bar{\zeta} = \left[\frac{4}{f''(0)}\right]^{1/3} BPr^{2/3}(1+m)\chi^{m+1/2}. \tag{60}$$

This regime must be avoided in this kind of transpiration cooling, due to the fact that the maximum temperature in the plate is very close to the temperature of the hot fluid in some parts of the plate. The resulting temperature gradients at the wall are also very high and are of the order of $(T_\infty - T_c)/h$.

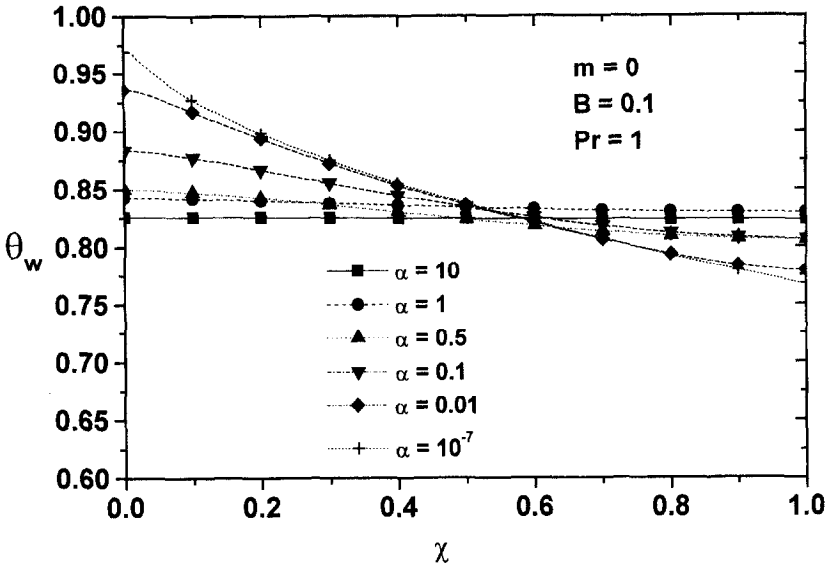

Fig. 7. – Nondimensional plate temperature as a function of the longitudinal coordinate for different values of the longitudinal heat conduction parameter α and $m = 0$. The injection strength is $B = 0.1$ and the Prandtl number is $\mathrm{Pr} = 1$.

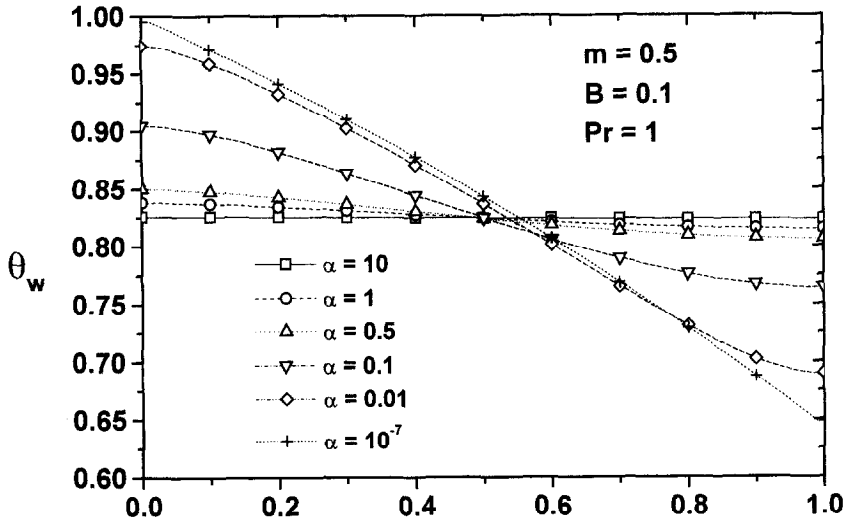

Fig. 8. – Nondimensional plate temperature as a function of the longitudinal coordinate for different values of the longitudinal heat conduction parameter α and $m = 1/2$. The injection strength is $B = 0.1$ and the Prandtl number is $\mathrm{Pr} = 1$.

5. Results

The nondimensional governing equations (17)–(21) were solved numerically using a quasilinearization technique with a tridiagonal matrix solver, employing a mesh of 101 and 900 grid points in the longitudinal (streamwise) and transverse directions in the fluid phase, respectively. Figures 7 and 8 show the nondimensional temperature distribution for different values of the parameter α, for $m = 0$ and $m = 1/2$, respectively. The injection strength assumed for these calculation was $B = 0.1$ and the Prandtl number was $Pr = 1$. For large values of the parameter α, the large thermal conductivity of the wall does not permit large temperature gradients and the temperature distribution is almost flat. As the value of α decreases, the temperature at the upstream

end increases, while it decreases at the downstream end, thus producing significant temperature gradients in the streamwise direction. The effect of m on the temperature distribution can be inferred from these two figures. For large values of α, the temperature of the wall is lower as the value of m increases, contrary to that expected. However, as the value of α decreases, the maximum temperature (at the upstream end) increases by increasing the value of m. All these trends can be obtained from the asymptotic solution, given in eq. (42). The nondimensional temperature at the upstream end, which is the location of the maximum temperature for $m > -1/2$, θ_{wl}, is according to eq. (42)

$$\theta_{wl} \cong 1 - \frac{\mathrm{Pr}\, B}{2G_{00}} - \frac{\mathrm{Pr}\, B^2}{2} H(m, \mathrm{Pr}, \alpha B), \tag{61}$$

where

$$H = -\frac{\mathrm{Pr}}{2G_{00}^2}\left(1 + \frac{2G_{01}(m, Pr)}{Pr}\right) - \frac{1}{\alpha B}\left[\frac{\widetilde{G_1}(m+2)}{(m+2)(m+5/2)} - \frac{\widetilde{G_1}(3/2)}{3}\right],$$

with $\widetilde{G}_1(n) = G_1(n)/G_{00}$. Here, all the parametric dependence is explicitly written. Differentiation of eq. (61) with respect to m gives

$$\frac{\partial \theta_{wl}}{\partial m} \cong \frac{\mathrm{Pr}\, B^2}{2}\left[\frac{1}{G_{00}^2}\frac{dG_{01}}{dm} + \frac{1}{\alpha B}\frac{d}{dm}\left(\frac{\widetilde{G_1}(m+2)}{(m+2)(m+5/2)}\right)\right], \tag{62}$$

or

$$\frac{\partial \theta_{wl}}{\partial m} \cong \frac{\mathrm{Pr}\, B^2}{2}\left[\frac{(-1.0487 + 0.872m)}{G_{00}^2} + \frac{4}{3\alpha B(m+5/2)}\int_0^1 \frac{u^{4m/3+5/3}du}{(1-u)^{1/3}}\left(\frac{4}{3}ln(1/u) + \frac{1}{(m+5/2)}\right)\right]. \tag{63}$$

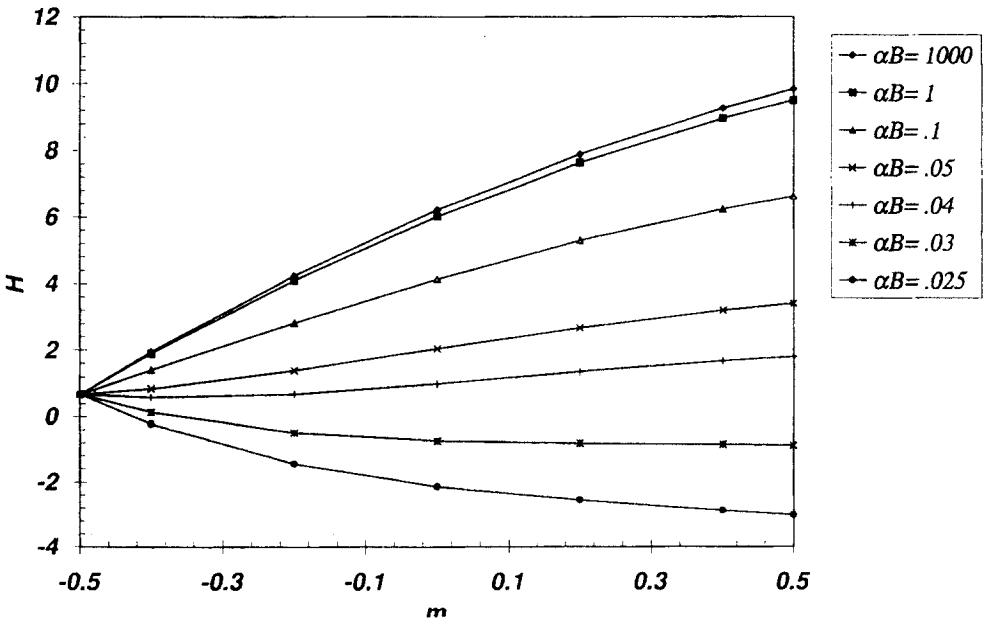

Fig. 9. – Values of H as a function of m for different values of αB and a Prandtl number of unity.

The first term in the right hand side of eq. (63) is negative, indicating that the temperature of the plate, to leading order, decreases as the value of m increases. On the other hand, the second term, showing the effect of α, is always positive, causing the temperature at the upstream end increase as the value of m increases, for $m > -1/2$. For values of $m < -1/2$, the temperature distribution on the plate inverts, being lower at the upstream end but with the highest temperature at the downstream end. Figure 9 shows H as a function of m, for different values of αB and $\mathrm{Pr} = 1$. Larger values of H imply a lower maximum temperature at the plate. For large values of α, increasing values of m gives higher values of H. However, for values of $\alpha B < 0.04$ the situation inverts, yielding lower temperatures for smaller values of m. In general, the numerical results are in good agreement with the asymptotic solution close to the asymptotic limits studied. Figure 10 shows the comparison of the nondimensional temperature distribution for two different values of m.

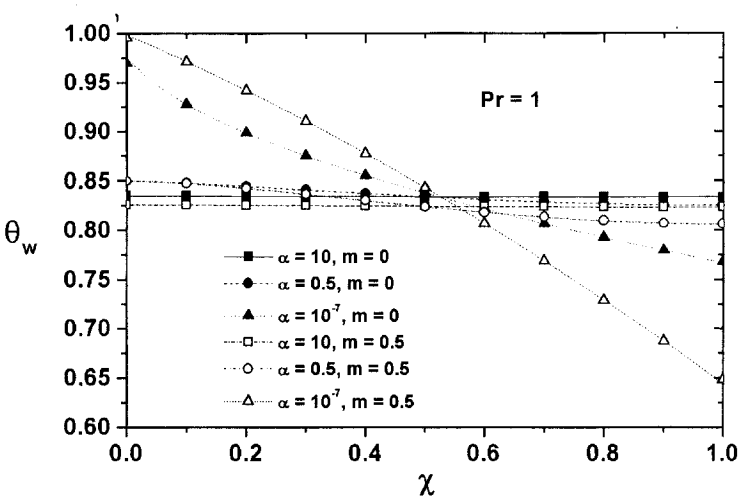

Fig. 10. – Effect of the parameter m on the distribution of the nondimensional temperature of the plate for three different values of α. The injection strength is $B = 0.1$ and the Prandtl number is $\mathrm{Pr} = 1$. It is to be noted that the adiabatic boundary conditions are satisfied for $\alpha = 10^{-7}$ at both ends. The plot is unable to resolve the very thin layer of order of $\alpha^{2/3}$ in χ.

6. Conclusions

In this paper we obtained asymptotic and numerical results for the steady-state transpiration cooling of a thin porous flat plate in a laminar hot convective flow, taking into account the streamwise heat conduction through the plate. The injection process is characterized by two nondimensional parameters: the injection strength and its distribution along the plate. In the thermally thin wall regime, the temperature variations in the transverse direction can be neglected. The aspect ratio of the plate (thickness to length) has no effect for thin plates in this regime. For highly conducting plates, a regular perturbation analysis has been performed, giving a three-term asymptotic solution for the distribution of the temperature in the plate. The maximum temperature is achieved at the upstream end for values of $m > -1/2$, which is most important from the practical point of view. This maximum temperature decreases with the value of m for very highly conducting plates, but increases with m as the value of α decreases. Using the data for typical material and flow conditions in gas turbines we find that the most common regime is the thermally thin wall regime with values of α of order unity. In the alternative limit of a very poorly conducting plate, a singular perturbation technique, based on matched asymptotic expansions, is employed to solve the governing equations. This limit is not of practical interest because the temperature at the upstream end is very close to that of the temperature of the hot stream.

Acknowledgments. – This work has been supported by the research grant IN107795, DGAPA at UNAM, Mexico. C. T. also acknowledges the support by CONACyT, through a *"Cátedra Patrimonial nivel II"* Fellowship.

REFERENCES

BROUWERS H. J. H., 1994, Heat Transfer between a fluid-saturated porous medium and a permeable wall with fluid injection and withrawal, *Int. J. Heat Mass Tran.*, **37**, 989–996.

BROUWERS H. J. H., 1995, Comments on "Transition from transpiration to film cooling", *Int. J. Heat Mass Tran.*, **38**, 183–184.

ECKERT E. R. G., CHO H. H., 1994, Transition from transpiration to film cooling, *Int. J. Heat Mass Tran.*, **37**, 3–8.

CHENG P., 1977, The influence of lateral mass flux on free convection boundary layers in a saturated porous medium, *Int. J. Heat Mass Tran.*, **20**, 201–206.

HARTNETT J. P., ECKERT E. R. G., 1957, Mass transfer cooling in a laminar boundary layer with constant fluid properties, *T. Am. Soc. Mech. Eng.*, **79**, 247–254.

HARTNETT J. P., BIRKEBAK R. G., ECKERT E. R. G., 1961, *Int. Dev. Heat Tran.*, Vol. IV, 682.

HIGUERA J. F., POP I., 1997, Conjugate natural convection heat transfer between two porous media separated by a vertical wall, *Int. J. Heat Mass Tran.*, **40**, 123.

LAI F. C., KULACKI F. A., 1990, The influence of surface mass flux on mixed convection over horizontal plates in saturated porous media, *Int. J. Heat Mass Tran.*, **33**, 576–579.

LIGHTHILL M. J., 1950, Contributions to the theory of heat transfer through a laminar boundary layer, *P. Roy. Soc. London*, **A202**, 359.

LUIKOV A. V., 1974, Conjugate convective heat transfer problems, *Int. J. Heat Mass Tran.*, **17**, 257–265.

MINKOWYCZ W. J., CHENG P., MOALEM F., 1985, The effect of surface mass transfer on buoyancy-induced Darcian flow adjacent to a horizontal heated plate, *Int. Comm. Heat Mass Tran.*, **12**, 55–65.

MODLIN J. M., COLWELL G. T., 1992, Surface cooling of scramjet engine inlets using pipe, transpiration and film cooling, *J. of Thermophys. Heat Tran.*, **6**, (3), 500.

PAYVAR P., 1977, Convective heat transfer to laminar flow over a plate of finite thickness, *Int. J. Heat Mass Tran.*, **20**, 431–433.

POLEZHAEV J., 1997, The transpiration cooling for blades of high temperatures gas turbine, *Energ. Convers. Manage.*, **38**, (10/13), 1123.

POZZI A., LUPO M., 1988, The coupling of conduction with laminar natural convection along a flat plate, *Int. J. Heat Mass Tran.*, **31**, 1807–1814.

SCHLICHTING H., 1979, *Boundary Layer Theory*, McGraw-Hill, New York.

SREEKANTH H., REDDY N. M., 1995, Study of transpiration cooling over a flat plate at hypersonic Mach numbers, *J. Thermophys. Heat Tran.*, **9**, (3), 552.

SHUNICHI U., 1996, two-dimensional numerical simulation of transpiration cooling system by outer/inner flow coupling, *Adv. Astronautical Sc.*, **91**, 81.

TREVIÑO C., LIÑÁN A., 1984, External heating of a flat plate in a convective flow, *Int. J. Heat Mass Tran.*, **27**, 1067–1073.

XU Y-H., YANG X-S., 1993, Control of transpiration cooling system and its characteristics, *Appl. Math. Mech.*, **14**, (11), 1047.

(Received 24 October 1997;
revised and accepted 12 November 1998.)